

## FASTER QUENCHING BY SILICON PULSED LASER ANNEALING UNDER WATER

A.POLMAN, S. ROORDA, S.B. OGALE\* and F.W. SARIS  
*FOM-Institute for Atomic and Molecular Physics  
Kruislaan 407, 1098 SJ Amsterdam, The Netherlands*

### ABSTRACT

*A novel method of pulsed laser processing of ion-implanted silicon is presented, in which samples are irradiated in water ambient. The water layer in contact with the silicon during irradiation has a considerable influence on melting and solidification dynamics. Still, perfect epitaxy of a thin amorphous layer can be obtained using this method.*

*For epitaxy to occur on a sample irradiated under water, 40 % more absorbed energy is necessary than for a sample irradiated in air. This indicates the occurrence of a considerable heat-flow from the silicon into the water layer during the laser pulse. From impurity redistribution after irradiation it is found that by processing a sample under water liquid-phase diffusion is reduced. Diffusion theory arguments indicate that this can be due to a reduction in total melt duration by about a factor 2-3. This can be due to faster cooling of the liquid silicon layer after the laser pulse whereas the melt-in time might be influenced as well. As a consequence, shallower impurity profiles can be obtained in crystalline silicon. No oxygen incorporation is detected and the surface morphology is not disturbed using this new process.*

### 1. INTRODUCTION

In recent years there has been considerable interest in pulsed laser processing of semiconductors for use in electronic or energy conversion devices<sup>1,2</sup>. In numerous situations pulsed laser irradiation is applied on thin ion-implanted silicon surface layers for impurity incorporation and epitaxial regrowth. At present, melting and resolidification processes are commonly understood from the results of extensive work on heat-flow phenomena and phase transformations involved. Impurity redistribution occurring during melting and solidification can generally be understood from mass diffusion and segregation arguments. Thus, by now, impurity profiles and structural state after irradiation can be predicted for given parameters such as laser energy density and pulse duration, laser wavelength absorption depth and thermodynamical properties of the material, mass diffusion and segregation coefficients for the specific dopants etc. Many intriguing aspects of pulsed laser irradiation such as explosive crystallization are still being explored<sup>3</sup>.

Pulsed laser irradiation is a promising technique to form shallow dopant profiles in low-energy implanted Si substrates due to the small laser skin depths and high quench rates. Irradiation at the threshold laser energy for melting through the amorphized layer results in epitaxial regrowth and in broadening of the dopant profile as a result of liquid-phase diffusion<sup>4</sup>. The total broadening obtained after irradiation is determined by the integral melt duration. If this duration could be reduced for the same melt depth, it would be possible to obtain shallower dopant profiles in epitaxially crystallized material.

In this paper we present a novel method of pulsed laser processing of ion implanted silicon, namely in water ambient. This technique is distinctly different as compared to the previously studied cases of laser irradiation in vacuum or in air. Here, the liquid on top of and in contact with the silicon surface acts as a heat sink, thus influencing the heat transfer processes within the sample. Whereas usually melting and solidification processes are governed only by heat diffusion into the bulk of the material, here also the water is used to deprive the surface layer of thermal energy. This has a considerable influence on melting and solidification dynamics and thus on impurity redistribution. As a consequence melt-depth and impurity redistribution can be

\*permanent address: Department of Physics, University of Poona, Pune - 411007, India

decoupled. For the same melt-depth shallower impurity profiles can be obtained, using this technique.

Experiments of laser irradiation in water ambient were performed on low-energy As implanted Si samples. From a study of the epitaxial regrowth process and of impurity redistribution, information is obtained concerning melting and solidification processes.

## 2. EXPERIMENTAL

Si <100> was implanted at room temperature by 10 keV As<sup>+</sup> ions to a dose of  $3 \times 10^{15} \text{ cm}^{-2}$ . Using this low implantation energy shallow impurity profiles are obtained. Arsenic is known to diffuse rapidly in liquid silicon on a nanosecond timescale and does not exhibit segregation effects at the liquid-solid interface under the present non-equilibrium conditions<sup>5,6</sup>. Pulsed laser irradiation was performed using a Q-switched ruby laser (wavelength 694 nm, pulse duration 32 ns FWHM). Laser energy was varied using volume-absorbing neutral density filters. A quartz guide diffusor<sup>7</sup> was used to obtain 5% uniformity over a 6 mm diameter spot. The mean energy density at the diffusor tube end was calibrated to within 3% using calorimetry.

The experimental set-up is shown schematically in Fig.1. Silicon samples were positioned in a glass beaker and then immersed in demineralized water at room temperature. To couple the laser energy into the sample the quartz diffusor was pinned through the water top surface. The water layer thickness above the sample surface was only 3 mm. Possibly some part of the energy guided through the diffusor is lost via the diffusor side walls under water. As the angular distribution of the light is unknown, it is not possible to exactly evaluate this energy loss. The critical angle for internal reflection within the diffusor in air is  $43^\circ$ , therefore at the sample position near the center of the diffusor end the change in energy density as a result of leakage through the side walls under water can be neglected. All samples were analysed near this center position upon irradiation. The final distance between exit surface and sample was 0.2 mm. In this way a well-defined quartz-water-Si layer structure was obtained. For a calculation of the amount of energy which is actually coupled into the silicon, taking into account reflectivity and absorption losses, this is of importance. Reference samples for irradiation in air were processed in the same configuration, before the water was poured in.

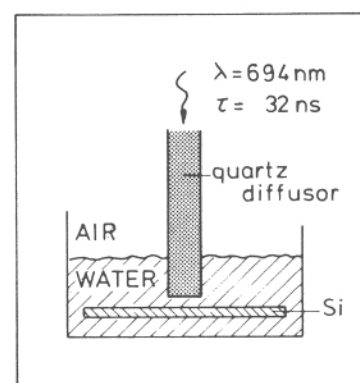


**Figure 1** Schematic representation of the experimental configuration.

Arsenic concentration profiles before and after irradiation were determined by Rutherford Backscattering Spectrometry (RBS)<sup>8</sup> using a 2 MeV He<sup>+</sup> beam in a random direction close to the surface normal. Reflected He particles were detected and energy-analysed by a surface barrier detector (energy resolution 14 keV) at a scattering angle of  $105^\circ$ , resulting in a depth resolution of  $\approx 150 \text{ \AA}$ . Channeling was employed to study the sample's structural state after irradiation. The threshold for surface melting was inferred from a colour change after irradiation due to the conversion of amorphous Si to poly-crystalline Si. A Scanning Electron Microscope (SEM) was employed to study the sample surface morphology before and after irradiation.

## 3. RESULTS

### 3.1 EPITAXY

Arsenic implanted samples were irradiated at an energy density in the range 0 - 1.5 J/cm<sup>2</sup>. Processing was done under water and in air. After irradiation, channeling RBS was employed on all samples to study the structure of the originally amorphous surface layer. All RBS

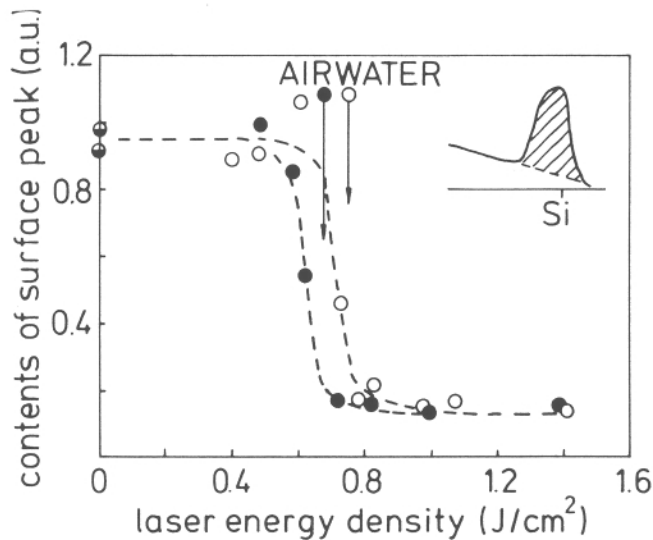


**Figure 2** Peak area in RBS channeling spectra as a function of energy-density in the diffusor end. Results for irradiation in water and in air are compared.

channeling spectra show a peak near the silicon surface backscattering energy. In Fig. 2 the peak area is shown for both samples processed in water (open circles) and in air (filled circles) as a function of the laser energy density in the quartz tube end. As can be seen, the peak area is high for energy densities below 0.7 and 0.6 J/cm<sup>2</sup> for the 'water' and 'air' cases respectively. The area corresponds to the originally amorphous layer thickness of  $\approx 250 \text{ \AA}$ . For high energy densities ( $> 0.9 \text{ J/cm}^2$ ) the peak area corresponds to the area of the surface peak of crystalline silicon. In the intermediate energy density range for both the 'water' and 'air' cases a sudden decrease in the peak area appears, indicating that epitaxial regrowth of the originally amorphous layer occurs above a specific threshold energy density. These thresholds obtained from interpolation in the figure are 0.77 J/cm<sup>2</sup> for treatment in water and 0.70 J/cm<sup>2</sup> for treatment in air respectively. Though the highly non-equilibrium heat transport processes occurring at the silicon-water interface are expected to influence the epitaxial regrowth process, a similar degree of crystal perfection (as far as detectable by RBS) is obtained under the two conditions of irradiation. This is evidenced by channeling measurements from a comparison of surface peak-area and minimum yield obtained on samples irradiated above the threshold for epitaxial regrowth.

Interesting conclusions can be obtained from a comparison between the absolute energy density thresholds for epitaxial regrowth. For such a comparison to be possible it should be studied first how the energy in the quartz diffusor is actually coupled into the silicon for both types of experimental conditions. Given the experimental configuration of Fig. 1 and the refractive indices of the media involved<sup>9</sup>, the effective transmission can be calculated. Table I represents the transmission into the silicon calculated using standard formulas for reflection and absorption at the two interfaces. High-order reflections, interference effects and absorption in water are neglected. Results depend on whether for silicon the liquid- or amorphous-phase parameters are employed. For low energy densities the silicon remains amorphous during most of the laser pulse, whereas for high energy densities the liquid phase will extend to nearly all over the pulse length. Thus two numbers can be calculated for the energy actually transmitted into the silicon (transmission  $T_a$  and  $T_l$  in Table I). At the threshold for epitaxial regrowth an intermediate value of  $T$  could be taken for both cases. Consequently it is found that for irradiation under water 28 % more energy is absorbed in the sample than for irradiation in air under comparable conditions. Yet, for irradiation under water still 10 % more energy from the laser is needed to obtain epitaxy, as follows from Fig. 2. Combining both numbers we see that 40 % more absorbed energy is necessary to obtain epitaxy on a sample immersed in water compared to a sample treated in air. This must be due to heat-diffusion from the silicon to

**Table I** Transmission into the silicon for the two experimental conditions. Results are given for amorphous-Si ( $T_a$ ) and liquid-Si ( $T_l$ ).

	quartz water Si	quartz air Si	ratio
$T_a$ (%)	69	56	1.23
$T_l$ (%)	33	25	1.32

the water during the laser pulse. A similar conclusion can be drawn from a comparison of the thresholds for surface melting under the two experimental conditions:  $0.63 \pm 0.03 \text{ J/cm}^2$  in water and  $0.59 \pm 0.03 \text{ J/cm}^2$  in air respectively. Taking into account the enhanced energy absorption of samples immersed in water, we see that  $30 \pm 15 \%$  more energy is necessary to melt the silicon surface layer in contact with the water layer.

### 3.2 ARSENIC DIFFUSION

Arsenic concentration profiles after irradiation were measured by RBS on all samples. Fig. 3 shows the Full Width at Half Maximum (FWHM) of As profiles as function of laser energy density in the end of the quartz tube. Results for samples treated in water and in air are compared. The thresholds for epitaxy (epi) are shown in the figure for the two cases. For all samples a broadening of As profiles is observed relative to the profile for an as-implanted sample ( $0 \text{ J/cm}^2$  in the figure).

First we will discuss the As peak width after irradiation in air (filled circles). For low energy densities ( $< 0.5 \text{ J/cm}^2$ ) the As peak width is only slightly above the detector resolution of 7 channels (indicated in the figure), therefore changes in the profile cannot accurately be detected. Between  $0.5$  and  $0.7 \text{ J/cm}^2$  the peak width increases significantly due to the increased meltdepth in the amorphous material. Above the threshold for epitaxy ( $0.7 \text{ J/cm}^2$ ) the melt depth is expected to increase further with energy density<sup>1,2</sup> and as a consequence we see a considerable increase in As peak width.

The As peak width behaviour after irradiation under water (open circles) is distinctly different from the behaviour described above. Upto the threshold for epitaxy only slight changes in the As profile are detected. The As peak width at the threshold for epitaxy is smaller than

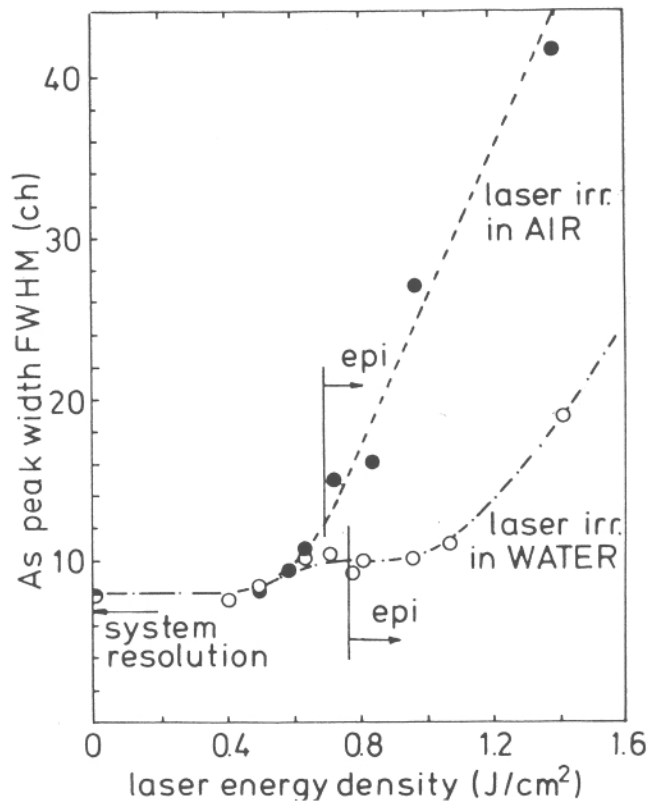


**Figure 3** FWHM width of As profiles obtained from RBS spectra without correction for the system resolution as a function of energy-density in the diffusor end. Results for irradiation in water and in air are compared.

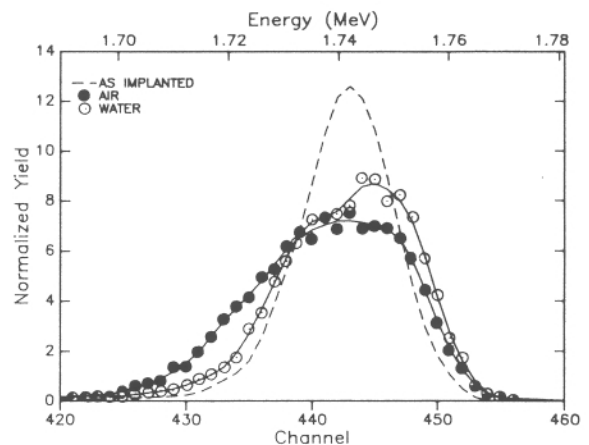


**Figure 4** RBS spectra of As profiles for two samples irradiated near the threshold energy density for epitaxial regrowth, in water (open circles) and in air (closed circles) respectively. A spectrum for an as-implanted sample is shown for reference (dashed line).

that at this threshold in case of irradiation in air. For higher energy densities the difference in As spreading between the two cases becomes even more distinct. Above the threshold for epitaxy the As peak width increases only slightly with energy density whereas for irradiation in air a fast increase is found.

Fig. 4 shows RBS spectra for two samples irradiated at an energy density very close to the threshold for epitaxy, in water and in air. A spectrum recorded from an as-implanted sample is shown for reference. At this threshold we expect the melt-depths to be equal under the two experimental conditions. Clearly a difference in As peak broadening, and thus As diffusion, between the two experimental cases can be seen. Especially the deep As tail visible at lower backscattering energies and the lower yield at the peak maximum for the sample irradiated in air are indicative for this. The increase in FWHM of the As concentration profiles, calculated after correction for the detector resolution corresponds to a distance of 110 Å in water and 170 Å in air respectively. In a model for spreading of the profiles we assume As diffusion to occur in liquid Si over a typical distance  $(Dt)^{1/2}$  where  $t$  is the total duration of the molten state and  $D$  the diffusion coefficient of As in liquid Si. Thus, as the total melt duration scales with the square of the profile broadening, we conclude that for irradiation in water the melt duration under conditions to obtain epitaxy is  $\approx 2$ -3 times shorter than for irradiation in air.

From these results we can conclude that the water layer has an influence on the heat-flow processes within the sample. Directly after the laser pulse has initiated a maximum melt depth, the liquid layer is deprived of thermal energy much faster than under comparable circumstances in air. Consequently the temperature of the liquid layer is reduced below the crystalline-Si melting temperature earlier, relative to the moment of maximum melt-penetration. This results in a shorter regrowth time. Apart from an influence on regrowth time, the heat exchange between silicon and water could also have an influence on the melt-in time, necessary for reaching the maximum melt-depth: the moment at which surface melting is initiated could be changed relative to the moment of maximum melt penetration. As both regrowth time and melt-in time contribute to the total melt-duration, the two effects as proposed here are of importance.

### 3.3 OXYGEN INCORPORATION AND SURFACE MORPHOLOGY

In earlier experiments of laser irradiation of Fe and Ti in water ambient it was found that large amounts of oxygen could be incorporated in the metal matrices<sup>10</sup>. Oxygen surface concentrations upto 70 % have been obtained with the profile extending to a depth of several 1000 Å. Therefore in the present experiments the oxygen content of the Si samples processed under water was determined. Integral oxygen concentrations were obtained from RBS channeling spectra in combination with suitable background subtraction. The total oxygen concentration is found to be similar for both samples irradiated in water and in air:  $4 \times 10^{15}$  atoms/cm<sup>2</sup>. This corresponds to a few mono-layers and shows that oxygen is not incorporated by laser processing under water<sup>11</sup>. The native oxide on the Si sample, present before irradiation, probably acts as a diffusion barrier for oxygen in-diffusion in the underlying molten silicon layer. This oxide has a higher melting temperature than crystalline Si.

The high thermal gradients at the silicon-water interface during melting and solidification might have an influence on the morphology of the sample surface. Therefore samples were analysed with a scanning electron microscope (SEM). No difference in surface morphology was found between samples irradiated in air and in water.

## 4. DISCUSSION

From the results presented in section 3.1 it follows that the heat transport from the heated Si layer to the originally room-temperature water layer is considerable. It is difficult to imagine how exactly this heat transport proceeds. Obviously the water temperature near the interface will increase significantly when such a considerable amount of energy is coupled from the silicon into the water. A characteristic distance  $d$  over which the heat will flow in the water during the laser pulse (duration  $\tau$ ) is determined by the heat capacity  $c_p$  and thermal conductivity  $\lambda$  at the proper temperature. At room temperature we find  $d = (\lambda\tau/c_p)^{1/2} \approx 100$

nm. In this layer thickness we thus expect the water to be heated considerably above its boiling point. Whether nucleation to the gas phase will occur on this nanosecond time scale or whether the water remains liquid in a superheated state can only be speculated upon, at present. No water bubbles were observed by eye during the experiment.

From the results in Section 3.2 it can be concluded that melt-depth and impurity redistribution can be decoupled, using this new technique. This is an advantage for shallow junction processing because deep implantation-tail damage annealing can be combined with reduced dopant diffusion.

## 5. CONCLUSIONS

The melting and solidification dynamics during laser irradiation of ion-implanted Si can be influenced by processing the sample immersed in water. A considerable heat-flow occurs from the silicon into the water layer during and after the nanosecond laser pulse. Still, perfect epitaxy of the amorphized layer is possible. A reduction in total melt duration by about a factor 2-3 is found when the sample is processed under water. This can be due to faster cooling of the liquid silicon layer after the laser pulse whereas the melt-in time might be influenced as well.

Using this method shallower impurity profiles can be obtained after annealing. No oxygen incorporation is detected and the surface morphology is not disturbed using this new process. Other liquids could be employed to further tailor the heat flow processes.

## ACKNOWLEDGEMENTS

René van Hal is gratefully acknowledged for his technical assistance in the experiments. Wijnand Takkenberg is acknowledged for the SEM analysis. Thanks are given to Arjen Vredenberg for illuminating discussions. This work is part of the research program of the Stichting voor Fundamenteel Onderzoek der Materie (FOM) and was financially supported by the Nederlandse Organisatie voor Zuiver Wetenschappelijk Onderzoek (ZWO).

## REFERENCES

- 1) *Laser Annealing of Semiconductors*, edited by J.M. Poate and J.W. Mayer (Academic Press, New York, 1982).
- 2) For a review of the current literature, see other volumes in this series, Mat. Res. Soc. Symp. Proc. **1**, **4**, **13**, **23**, **35**, **51** (1981-1986)
- 3) J.J.P. Bruines, R.P.M. van Hal and H.M.J. Boots, A.Polman and F.W. Saris, Appl. Phys. Lett. **49**, 1161 (1986)
- 4) C.W. White, P.P. Pronko, S.R. Wilson, B.R. Appleton, J. Narayan and R.T. Young, J. Appl. Phys. **50**, 3261 (1979)
- 5) J. Narayan, C.W. White, O.W. Holland and M.J. Aziz, J. Appl. Phys. **56**, 1821 (1984)
- 6) S.H. Kodera, Jap. J. Appl. Phys. **2**, 212 (1965)
- 7) A.G. Cullis, H.C. Webber and P. Bailey, J.Phys.E: Sci. Instrum. **12** (1979) 688
- 8) *Backscattering Spectrometry*, W.-K. Chu, J.W. Mayer and M.-A. Nicolet (Academic Press, New York, 1978)
- 9) *Semiconductors and Semimetals*, Vol. **23**, *Pulsed laser Processing of Semiconductors*, edited by R.F. Wood, C. White and R.T. Young (Mc Graw Hill, New York, 1984)
- 10) S.B. Ogale, A.Polman, F.O.P. Quentin, S.Roorda and F.W. Saris, accepted for publication in Appl. Phys. Lett.
- 11) Z.L. Wang, J.F.M. Westendorp and F.W. Saris, Nucl. Instr. Meth. **211** (1983) 193